



HAL
open science

Nonsingular change of assembly mode without any cusp

Michel Coste, Damien Chablat, Philippe Wenger

► **To cite this version:**

Michel Coste, Damien Chablat, Philippe Wenger. Nonsingular change of assembly mode without any cusp. Jadran Lenarcic; Oussama Khatib. *Advances in Robot Kinematics*, Springer, pp.105-112, 2014, 978-3-319-06697-4. 10.1007/978-3-319-06698-1_12 . hal-00959842

HAL Id: hal-00959842

<https://hal.science/hal-00959842v1>

Submitted on 17 Mar 2014

HAL is a multi-disciplinary open access archive for the deposit and dissemination of scientific research documents, whether they are published or not. The documents may come from teaching and research institutions in France or abroad, or from public or private research centers.

L'archive ouverte pluridisciplinaire **HAL**, est destinée au dépôt et à la diffusion de documents scientifiques de niveau recherche, publiés ou non, émanant des établissements d'enseignement et de recherche français ou étrangers, des laboratoires publics ou privés.

Nonsingular change of assembly mode without any cusp

Michel Coste, Damien Chablat and Philippe Wenger

Abstract This paper shows for the first time a parallel manipulator that can execute nonsingular changes of assembly modes while its joint space is free of cusp points and cuspidal edges. The manipulator at hand has two degrees of freedom and is derived from a 3-RPR manipulator; the shape of its joint space is a thickening of a figure-eight curve. A few explanations concerning the relationship between cusps and alpha curves are given.

Key words: parallel robots, singularities.

1 Introduction

The nonsingular change of assembly mode in parallel manipulators was first observed by C. Innocenti and V. Parenti-Castelli [1]. The possibility to execute such a motion is most frequently associated with the presence of cusps, and the nonsingular change of assembly mode is realized by turning around a cusp point, or a cuspidal edge of the singularity surface (see for instance [2, 3, 4, 5]). It has also been reported [6, 7] that nonsingular change of assembly modes can be realized by following an “alpha curve” (i.e. a fold curve intersecting itself transversally) but, in the examples shown, such an alpha curve is always associated with the presence of cusps. Figure 1 shows such an example. The figure depicts a slice of the joint space for a 3-RPR manipulator, along with a nonsingular assembly mode changing trajectory that goes around the alpha-curve. The zone with four (resp. two) solutions to

Michel Coste
IRMAR, Université de Rennes 1 – CNRS, e-mail: michel.coste@univ-rennes1.fr
Damien Chablat
IRCCyN, CNRS – École Centrale de Nantes, e-mail: damien.chablat@irccyn.ec-nantes.fr
Philippe Wenger
IRCCyN, CNRS – École Centrale de Nantes, e-mail: philippe.wenger@irccyn.ec-nantes.fr

the direct kinematic problem is colored in green (resp. red). Going from the green zone to the green zone following the trajectory, one passes from one solution to the other solution in the same aspect. Since there are two cusps, note that a nonsingular change of assembly mode may also be executed by encircling one of them.

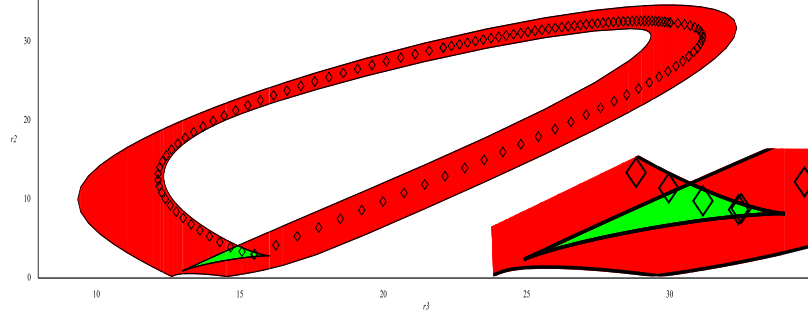


Fig. 1 Change of assembly mode looping around an alpha curve, with a zoom on the zone with four solutions to the direct kinematic problem

In the present paper we describe a planar parallel manipulator with two degrees of freedom which has absolutely no cusp, but nevertheless allows nonsingular changes of assembly modes. This manipulator is derived from a 3-RPR manipulator with one prismatic articulation blocked, coupled with a mechanism for reversing an angle. We describe this manipulator in the next section. The idea behind the special design of this manipulator is to obtain a joint space which has the shape of a thickened figure-eight curve. This is first established with an asymptotic simplification of the inverse kinematic mapping in section 3. Section 4 contains the actual example of a nonsingular change of assembly mode showing no cusp at all. Some remarks on stable singularities are given in section 5; in particular, we comment about the relationship between cusps and alpha curves.

2 The non cuspidal manipulator

The manipulator we describe here derives from a planar 3-RPR. It has a triangular moving platform $B_1B_2B_3$ which is linked to the base $A_1A_2A_3$ via three legs A_iB_i , with passive rotoidal joints at A_i and B_i (for $i = 1, 2, 3$). The length r_1 of the leg A_1B_1 is fixed. The lengths r_2 and r_3 of the other two legs A_2B_2 and A_3B_3 are controlled by actuated prismatic joints. The vertices A_1 and A_2 of the base are fixed. The length A_1A_3 is fixed. The peculiarity of this manipulator, which makes it different from a 3-RPR with one blocked prismatic joint, is the fact that the angle $\widehat{A_2A_1A_3}$ varies.

Precisely, if we denote by θ the angle $\widehat{A_2A_1B_1}$, then $\widehat{A_2A_1A_3} = \frac{\pi}{2} - \theta$ (see Figure 2).

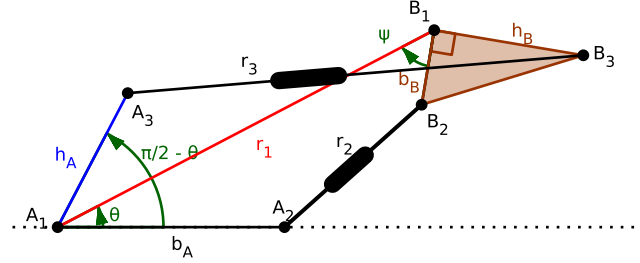


Fig. 2 The manipulator

Let us complete the description of the manipulator. The platform $B_1B_2B_3$ is a right-angled triangle, with right angle at B_1 . Its dimensions are given by $b_B = B_1B_2$ and $h_B = B_1B_3$. The dimensions of the base are given by $b_A = A_1A_2$ and $h_A = A_1A_3$. The position of the manipulator is completely described by the angles θ and $\psi = \widehat{B_2B_1A_1}$.

We explain now how one can constrain the angle $\widehat{A_2A_1A_3}$ to be equal to $\frac{\pi}{2} - \theta$. Consider a 4-bar kite A_1CDE with $A_1C = A_1E$ and $CD = ED$. The rotoidal joint A_1 is fixed and D is constrained to glide on A_1A_2 . The rotoidal joint E is on the leg A_1B_1 . Of course, we have $\widehat{A_2A_1C} = -\theta$. We constrain A_1A_3 to be orthogonal to A_1C so that $\widehat{A_2A_1A_3} = \frac{\pi}{2} - \theta$ (see Figure 3, left).

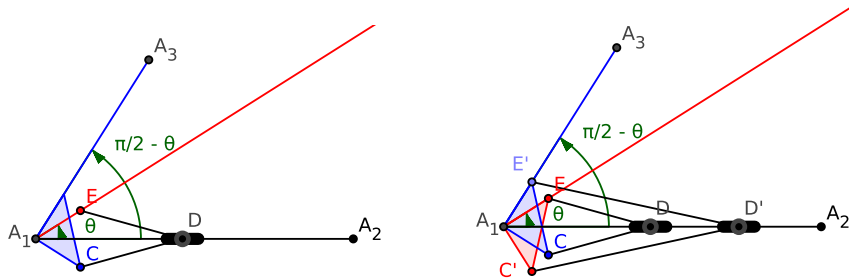


Fig. 3 The 4-bar kite and the two coupled kites

When the 4-bar kite is flat (this happens when $\theta = 0$ or π), it can change its operating mode by moving in such a way that C and E remain coincident. In order to rule out this possibility, we can couple the first kite A_1CDE with a second one $A_1C'D'E'$, as shown on Figure 3, right.

We could have used other mechanisms in order to reverse the angle θ : for instance Kempe's reverser consisting of two contra-parallelograms (see [8] p.270), or belts, or gears.

3 The inverse kinematic mapping and its asymptotic simplification

The constraint equations of the manipulator can be written as follows. Recall that r_i is the length of the leg A_iB_i . The actuated joint variables are r_2 and r_3 , while r_1 is fixed. The position of the manipulator is determined by the angles θ and ψ . We have:

$$\begin{aligned} r_2^2 &= (r_1 - b_A \cos \theta - b_B \cos \psi)^2 + (b_A \sin \theta + b_B \sin \psi)^2, \\ r_3^2 &= (r_1 - h_A \sin 2\theta - h_B \sin \psi)^2 + (h_A \cos 2\theta + h_B \cos \psi)^2. \end{aligned} \quad (1)$$

Equations (1) describe the inverse kinematic mapping from the workspace, which is a torus parametrized by the angles θ and ψ , to the actuated joint space, which is the positive quadrant parametrized by the lengths r_2 and r_3 .

We shall now consider the asymptotic version of the inverse kinematic mapping as r_1 tends to infinity, as was done in [9] for the usual 3-RPR manipulator. In order to do this, we replace r_2 and r_3 with $r_2 - r_1$ and $r_3 - r_2$ and take their limit $\delta_i = \lim_{r_1 \rightarrow \infty} (r_i - r_1)$ for $i = 2, 3$. We obtain:

$$\begin{aligned} \delta_2 &= -b_A \cos \theta - b_B \cos \psi, \\ \delta_3 &= -h_A \sin 2\theta - h_B \sin \psi. \end{aligned} \quad (2)$$

Equations (2) describe the asymptotic simplification of the inverse kinematic mapping, from the torus (θ, ψ) to the plane (δ_2, δ_3) . The singularities of the asymptotic inverse kinematic mapping are easily understood. Remark that $(b_A \cos \theta, h_A \sin 2\theta)$ is a parametrization of a figure-eight curve, or lemniscate of Gerono (a particular case of a Lissajous curve), while $(b_B \cos \psi, h_B \sin \psi)$ is, of course, the parametrization of an ellipse. So the curve of critical values of the asymptotic inverse kinematic mapping is the envelope of a family of translated ellipses with centres on a figure-eight curve. If the ellipse is small compared to the figure-eight curve, we obtain just a thickening of the figure-eight curve.

Specifically, take $b_A = 10$, $h_A = 5$, $b_B = 1$, $h_B = 2$. The Jacobian determinant of the asymptotic inverse kinematic mapping is then

$$J = -20 \sin \theta \cos \psi + 10 \cos 2\theta \sin \psi. \quad (3)$$

Solving $J = 0$ for ψ , we obtain that the critical points of the asymptotic inverse kinematic mapping are those such that

$$\cos \psi = \frac{\pm \cos 2\theta}{\sqrt{1 + 4 \sin^4 \theta}}, \quad \sin \psi = \frac{\pm 2 \sin \theta}{\sqrt{1 + 4 \sin^4 \theta}}. \quad (4)$$

The two branches of the curve of critical points in the (θ, ψ) torus are represented in thick black line in Figure 4, left. These two branches delimit two aspects.

Carrying these values in the equations (2) for the asymptotic inverse kinematic mapping, we get the two branches of the curve of critical values in the (δ_2, δ_3) plane. They are represented in Figure 4, right. These curves delimit zones where the direct kinematic problem has two solutions (red zone), and four solutions (green zone).

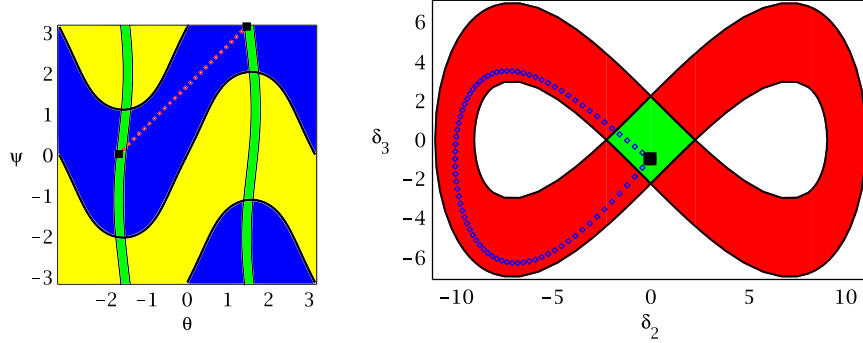


Fig. 4 Work space: the (θ, ψ) torus (left) and joint space: the (δ_2, δ_3) plane (right) for the asymptotic model

There is no cusp, but a nonsingular change of assembly mode is possible since there are two aspects and a zone where the direct kinematic problem has four solutions. A trajectory for such a nonsingular change of assembly mode is represented in Figure 4. The nonsingular change of assembly mode can be interpreted using a comparison with a figure-eight race track where the crossroads is realized with a bridge, i.e. there are two levels at the crossroads. Each level is associated with an assembly mode. The track represents an aspect (the joint space is made of two superimposed similar aspects). Starting from the crossroads on the bridge (level 1), the car can drive until it reaches the crossroads at the same horizontal position but under the bridge (level 0).

The characteristic curves have been plotted in thin black line in Figure 4, left. These curves, together with the critical curves, define the uniqueness domains: any two points in the same uniqueness domain of the (θ, ψ) torus have different images in the (δ_1, δ_2) plane (joint space). For a complete definition of the characteristic surfaces and uniqueness domains, see [10]. Any point in the green region of the joint space (Figure 4, right) is the image of four points in the workspace (four assembly modes). These four points are distributed in the four green regions shown in the workspace (Figure 4, left), two in each aspect.

The preceding analysis concerns, of course, only an asymptotic case. However, since the asymptotic inverse kinematic mapping has only stable singularities (folds and transverse intersection of folds, see Section 5) which are not altered by small perturbations, the conclusion obtained will remain valid for all sufficiently large values of r_1 . We shall check this in the next section.

4 An actual, non asymptotic example

The asymptotic analysis of the preceding section corresponds to $r_1 = \infty$. We show here that the conclusion remains valid for $r_1 = 30$ (keeping the same b_A, h_A, b_B, h_B). We have now to deal with equations (1) which are more complicated than their asymptotic simplification. The computation is done using the SIROPA library. In order to simplify calculations, we use coordinates $l_2 = r_2^2, l_3 = r_3^2$ for the actuated joint space, which is an unessential change.

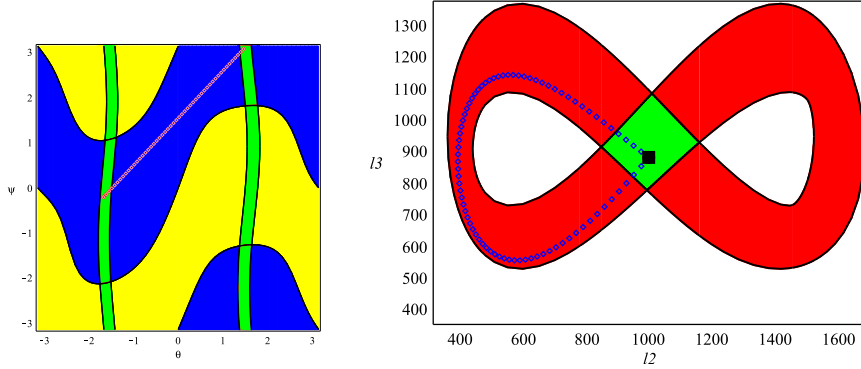


Fig. 5 Workspace and joint space for $r_1 = 30$, with a nonsingular change of assembly mode

We can see on Figure 5 that the picture of the singularities is the same as the one for the asymptotic simplification (Figure 4). In particular, there is no cusp. We have also represented a nonsingular trajectory between two configurations corresponding to the same values $l_2 = 1000, l_3 = 880$ for the actuated joints.

5 Stable singularities and nonsingular change of assembly modes

The only stable singularities of a mapping from a surface to a surface (see [11]) are the folds (codimension one singularity, giving a fold curve), the cusps and the transverse intersections of fold curves (codimension two singularities, i.e. isolated points). Any other singularity will be decomposed into a combination of these stable singularities by a small perturbation, whereas a stable singularity is persistent under small perturbations.

Figure 6 represents these three stable singularities for a critical value P . Generically, the picture of parallel singularities in a two-dimensional surface around a critical value of the inverse kinematic mapping in the joint space will fit into one of these three cases. The direct kinematic problem has a double solution for a fold, a triple solution for a cusp and two double solutions for a transverse intersection of fold curves.

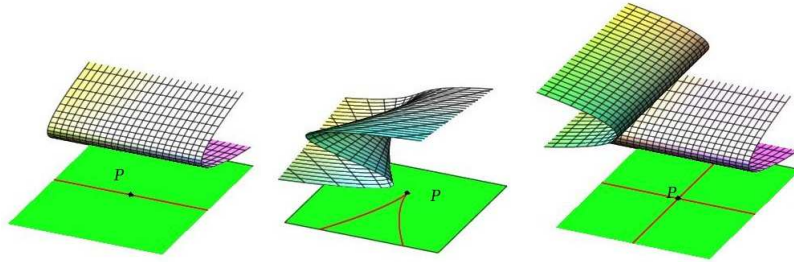


Fig. 6 Stable singularities: fold, cusp and transverse intersection of fold curves

The only stable singularity which allows *local* nonsingular change of assembly mode is the cusp. By “local”, we mean that the change of assembly mode is performed by following a loop which can be shrunk to become arbitrarily small. This is certainly the case for a loop encircling a cusp, but not for a loop following an “alpha curve”, i.e. a fold curve intersecting itself transversally.

In examples, an alpha curve is frequently associated with cusps because a transversal intersection of folds often appears after a “swallowtail bifurcation” (see [12] p. 34), together with a pair of cusps. One might think that a cusp is obtained by shrinking the loop of an alpha curve to a point. This is not the case, since a cusp is a stable singularity which cannot be obtained by degenerating another singularity. If the loop of an alpha curve is shrunk to a point, then this point corresponds to a quadruple, not triple, solution to the direct kinematic problem.

In order to illustrate an example of degeneration of an alpha curve, and also the swallowtail bifurcation, we show the transformation of the (δ_2, δ_3) joint space of section 3, as we decrease h_A keeping the other dimensions fixed. Only a half of the joint space is shown in Figure 7, since it is symmetric.

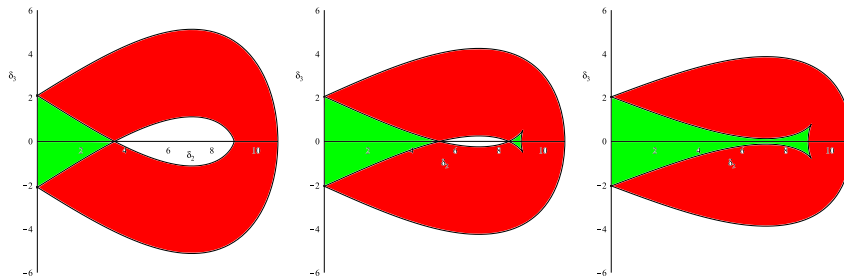


Fig. 7 Degeneration of an alpha curve

Figure 7 shows that, at first, two cusps and a transverse intersection of fold curves appear as a result of a swallowtail bifurcation. Then, the two transverse intersections of fold curves disappear through a tangent crossing of these curves.

6 Conclusion

While it is clear that the existence of cusps or cuspidal edges is a sufficient condition for allowing a nonsingular change of assembly mode, the question of whether this condition is necessary or not remained to be fixed because previous examples of nonsingular assembly mode changing manipulators always exhibited cusps, even in the presence of an alpha-curve. This paper showed that the aforementioned condition is indeed not necessary, through the presentation of a 2-DOF parallel manipulator that can execute a nonsingular change of assembly mode while its joint space is free of cusps. This manipulator is derived from a 3-RPR and its joint space is a thickening of a figure-eight curve. The kinematic properties of this manipulator were first established using the asymptotic simplification of its inverse kinematic mapping.

It was recalled that a cusp is a necessary and sufficient condition for *local* nonsingular change of assembly mode in generic situations; it was also explained that a cusp cannot be interpreted as a degeneration of an alpha-curve.

References

1. C. Innocenti and V. Parenti-Castelli, "Singularity-free evolution from one configuration to another in serial and fully-parallel manipulators?", *J. Mech. Des.*, 120: 73-79 (1998)
2. P.R. McAree and R.W. Daniel, "An explanation of never-special assembly changing motions for 3-3 parallel manipulators", *The International Journal of Robotics Research*, 18(6): 556-574 (1999)
3. M. Zein, P. Wenger and D. Chablat, "Singular curves in the joint space and cusp points of 3-RPR parallel manipulators", *Robotica*, 25(6): 717-724 (2007)
4. S. Caro, P. Wenger and D. Chablat, "Non-singular assembly mode changing trajectories of a 6-DOF parallel robot". In: *Proceedings of the ASME 2012 International Design Engineering Technical Conferences & Computers and Information in Engineering Conference IDETC/CIE 2012*, pp 1245-1254, 2012.
5. M. Husty, J. Schadlbauer, S. Caro and P. Wenger, "The 3-RPS manipulator can have nonsingular assembly-mode changes". In: *Computational Kinematics, Mechanisms and Machine Science* Vol. 15, pp 339-348. Springer (2014)
6. H. Bamberger, A. Wolf and M. Shoham, "Assembly mode changing in parallel mechanisms", *IEEE Transactions on Robotics*, 24(4): 765-772 (2008)
7. E. Macho, O. Altuzarra, C. Pinto and A. Hernandez, "Transitions between multiple solutions of the direct kinematic problem". In: *Advances in Robot Kinematics: Analysis and Design*, pp 301-310. Springer (2008)
8. G. Koenigs, *Leçons de cinématique*. Hermann (1897)
9. M. Coste, "Asymptotic singularities of planar parallel 3-RPR manipulators". In: *Latest Advances in Robot Kinematics*, pp 35-42. Springer (2012)
10. P. Wenger and D. Chablat, "Uniqueness domains in the workspace of parallel manipulators". In: *I.F.A.C. Symposium on Robot Control (SYROCO'97)*, pp 431-436 (1997)
11. H. Whitney, "On singularities of mappings of Euclidean spaces, I. Mapping of the plane into the plane" *Annals of Mathematics* 62(3): 374-410 (1955)
12. V.I. Arnol'd, *Catastrophe theory*. Springer (1992)